Chinese Chemical Letters 34 (2023) 108412

Contents lists available at ScienceDirect

Chinese Chemical Letters

journal homepage: www.elsevier.com/locate/cclet

Photo-catalytic *Staphylococcus aureus* inactivation and biofilm destruction with novel bis-tridentate iridium(III) photocatalyst

Shihao Chen[a,1], Zhishang Zhang[b,1], Li Wei[b], Zhongxian Fan[b], Yue Li[c], Xuezhi Wang[a], Tongming Feng[a,*], Huaiyi Huang[b,*]

[a] The Fourth People's Hospital of Foshan, Foshan 528000, China
[b] School of Pharmaceutical Science (Shenzhen), Shenzhen Campus of Sun Yat-sen University, Shenzhen 518107, China
[c] College of Chemistry and Environmental Engineering, Shenzhen University, Shenzhen 518060, China

ARTICLE INFO

Article history:
Received 15 November 2022
Revised 28 March 2023
Accepted 30 March 2023
Available online 31 March 2023

Keywords:
Ir(III) photocatalyst
NADH depletion
Reactive oxygen species
Antimicrobial photocatalytic therapy

ABSTRACT

Bacterial infection is currently a serious challenge globally, causing death of thousands of human beings. New antimicrobial agents with novel mechanism of action are urgently needed. Transition metal complexes have shown great potentials in photodynamic and photocatalytic therapy. Herein, we take full advantage of metal photocatalyst and successfully developed a novel cyclometalated iridium(III) complex (**Ir1**) with higher biofilm damage efficiency than the clinical antibiotics. **Ir1** synergistically generates reactive oxygen species and coenzyme photocatalytic activity with high efficiency under white light irradiation. Combined with these properties, **Ir1** exhibited excellent photoinactivation of *S. aureus* and effectively damaged the biofilm. This work provides a new approach for the development of antibacterial photodynamic therapy.

The discovery of organic antibiotics several decades ago has dramatically reduced the death caused by bacterial infections [1]. However, due to the abuse of antibiotics, multidrug-resistant bacteria have emerged and threatened thousands of human's health around the world nowadays [2]. For example, the methicillin-resistant *Staphylococcus aureus* (*S. aureus*) is a common type of hospitalization infectious bacteria that shows resistance to several antibiotics [3]. Thus, it is important to investigate antimicrobial agents with novel mechanism of action (MoA).

All the time, transition metal complexes are widely used in cancer diagnosis and treatment [4–7], which arises people to explore their effectiveness to antibacterial. Therefore, in addition to the traditional organic antibiotic, transition metal complexes which exhibit inherent phosphorescent and readily tunable photophysicochemical properties have been reported to combat the severe drug-resistant bacterial. Collins's group discovered several series of polynuclear complexes Ru(II) complexes for antimicrobial application *via* intercalating with nucleic acids [8,9]. On the other hand, iridium complexes have also been discovered as potential antibacterial agents. In 2018, Sadler *et al.* synthesized Ir(III) complexes with metformin which showed antimicrobial activity [10]. In addition, Sasmal *et al.* reported a series of cyclometalated Ir(III) complexes with simultaneous ultrasensitive detection properties to eliminate drug-resistant bacteria [11]. However, the above metal complexes function as antimicrobial chemotherapeutic drugs lacking spat-temporal selectivity and thus may induce side effects.

Antimicrobial photodynamic therapy (APDT) has been recognized as a promising therapeutic, providing patio-temporal control over drug activation to inactive bacteria. Upon light activation, APDT uses photosensitizers (PSs) to generate diverse reactive oxygen species (ROS) to induced intracellular oxidative damage *via* two main pathways. The type I pathway includes electron transfer between the excited state PS with substrate and oxygen at the ground states, generating diverse radicals and superoxide anion. Type II pathway involves direct energy transfer from excited state PS to oxygen, producing the highly reactive singlet oxygen [12]. Currently, photosensitizers applied for antibacterial mainly include type II organic photosensitizers, such as porphyrin [13], 4,4-difluoro-boradiazaindacene (BODIPY) [14] and aggregation-induced emission PSs analogues [15]. However, the poor water solubility and high oxygen dependent MoA limited their applications. It is important to mention that metal PSs are rarely investigated in antimicrobial photo-therapy. Only until recently, Sadler and co-workers reported a photoactivatable Ru(II)-isoniazid complex consist of the labile coordinated antimicrobial drug isoniazid

* Corresponding authors.
E-mail addresses: 13702446638@139.com (T. Feng), huanghy87@mail.sysu.edu.cn (H. Huang).
[1] These authors contributed equally to this work.

https://doi.org/10.1016/j.cclet.2023.108412
1001-8417/

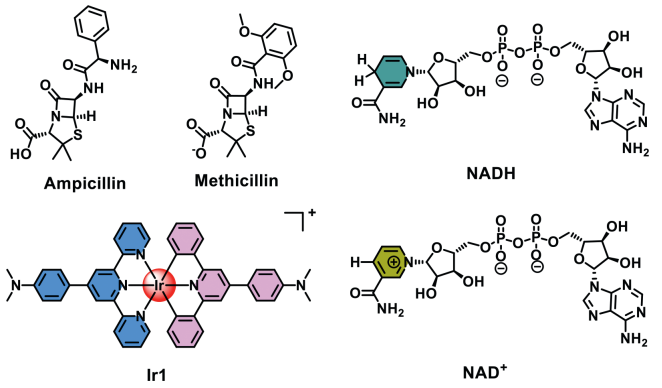

Scheme 1. The chemical structure of antibiotics, NADH, NAD^+ and the bis-tridentate Ir(III) photocatalyst used in this study.

for mycobacteria [16]. Chen and coworkers reported Ir(III) complexes targeting negatively charged bacterial membrane, despite extremely high light dose required (white light, 484.2 J/cm^2) [17]. It is necessary to mention that the above mentioned metal PSs did not or can only slightly inhibit the capability of antibiofilm. Therefore, developing highly efficient metal complexes with the ability to destruct biofilms are urgently needed.

Our group previously reported tri-dentate Ir(III) photocatalysts exhibited high photocatalytic activity for coenzyme I, the reduced nicotinamide adenine di-nucleotide (NADH), as novel photocatalytic mechanism for phototherapeutics. NADH participates in the maintenance of intracellular redox balance, and as a coenzyme for cellular oxidoreductases [18]. However, the APDT application of bis-tridentate Ir(III) photocatalysts were seldom reported. Herein, we reported a novel Ir(III) photocatalyst (**Ir1**) (Scheme 1) for synergistically photodynamic and photocatalytic antimicrobial therapy. **Ir1** effectively inactivated Gram-positive *S. aureus via* generating diverse ROS and photocatalytic oxidation of NADH under low light dose (21.1 J/cm^2). Importantly, **Ir1** damaged the cell membrane of *S. aureus* leading to protein leakage and showed stronger ability to damage the biofilm capability than the clinical used antibiotic.

The synthetic routes for the tridentate ligands and **Ir1** were shown in Scheme S1 (Supporting information) with slightly modification from literature [19]. **Ir1** was characterized by ^{1}H NMR, ^{13}C NMR and HRMS (Figs. S1 and S2 in Supporting information). Notably, the positive-charged **Ir1** may improve the potent interaction with the negatively charged bacterial membrane [11]. The absorption and photoluminescent spectra of **Ir1** were depicted in Figs. 1a and b. Differ from the widely studied tri-bidentate Ir(III) complexes, **Ir1** exhibited extended absorption bands tailing to 600 nm and emit intense deep-red phosphorescence (λ_{max} = 685 nm) [20]. Importantly, the phosphorescent intensity enhanced about 3-fold in the absence of oxygen, indicating strong interaction between the excited state of **Ir1** and the molecular oxygen (Fig. 1b). In view of the absorbance spectrum of **Ir1**, the white light source was employed to trigger the photo-induced activity in phosphate buffer solution (PBS) buffer solution.

The dark- and photo-stability are two important factors for a potent photosensitizer candidate to avoid off-target dark toxicity and photo-degradation. **Ir1** exhibited higher photostability than the widely used organic PS chlorin e6 (Ce6), as evaluated by the time-dependent UV–vis spectra under continuous light irradiation (Fig. 1c). The singlet oxygen generation ability (type II energy transfer pathway) of **Ir1** was detected by 9,10-anthracenediyl-bis(methylene) dimalonic acid (ABDA) [21]. Upon white light irradiation, the absorbance of ABDA decreased readily (Fig. 1d), compared with the standard metal PS $[Ru(bpy)_3]^{2+}$ (Fig. S7 in Supporting information). Since superoxide anion can inactive bacteria

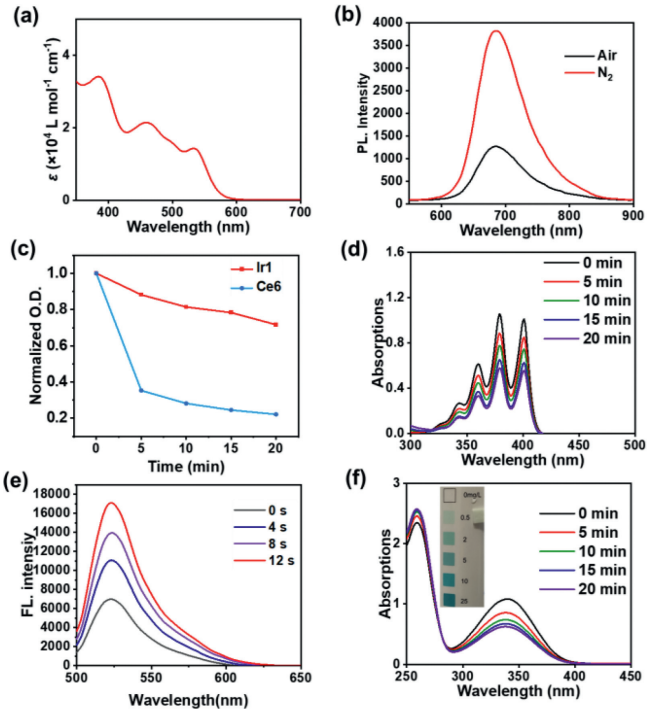

Fig. 1. Photophysical and photochemical properties of **Ir1**. (a) Absorption spectra of **Ir1** in CH_2Cl_2. (b) Phosphorescence spectra of **Ir1** in CH_2Cl_2 at 298 K, λ_{ex} = 525 nm. (c) Photo-stability of **Ir1** and Ce6. (d) ABDA photodegradation by **Ir1**. (e) Change of fluorescent intensity of DHR123 by **Ir1**. (f) Photocatalytic oxidation of NADH by **Ir1**. Insert: H_2O_2 production after white light exposure.

via type I electron transfer pathway [22]. Thus we detected the superoxide anion generation efficiency with a fluorescent sensor dihydrorhodamine 123 (DHR123) [23]. As shown in Fig. 1e, after extremely short white light irradiation (4 s), DHR123 was rapidly oxidized and generated the highly fluorescent rhodamine 123. Especially, when irradiated for 12 s, the fluorescent intensity enhanced 3-fold, indicating high superoxide anion generation ability of **Ir1**.

We previously reported that Ir(III) PSs can catalyze cellular NADH oxidation upon light irradiation and induce intracellular redox imbalance [24,25]. Thus, we explored the NADH catalytic activity of **Ir1**. In the absence of light, the absorbance of NADH remained unchanged with **Ir1** (Fig. S6 in Supporting information). After 5 min white light irradiation, significant decrease of absorbance at 339 nm was observed, indicating effective depletion of NADH (TOF = 219.9 h^{-1}, Fig. 1f). This property might be a critical factor for antibacterial activity, since NADH plays an important role in cell metabolism of living bacteria [18]. Moreover, H_2O_2 generation was detected by H_2O_2 test paper during NADH photocatalysis (Fig. 1f, inserted photograph). The above results indicated that **Ir1** can generate diverse ROS and oxidized NADH upon white light activation.

The excellent photosensitization and photocatalytic activity of **Ir1** promoted us to investigate the antimicrobial activity toward typical bacteria such as the Gram-positive bacteria (*S. aureus*), the Gram-negative bacteria *E. coli* (*E. coli*) and *Mycolicibacterium smegmatis* (*M. smegmetis*). The antibiotic used in clinic such as ampicillin, methicillin and streptomycin (Scheme 1) were tested as well. The minimum inhibitory concentration (MIC_{90}) was defined. After incubating with **Ir1** for 4 h, the bacteria were either kept in the dark or received white light irradiation (21.1 J/cm^2), following by 14 h incubation in the dark. The survival rates of bacteria after dark or light treatment were shown in Figs. 2a and b and Fig. S8 (Supporting information). The light MIC_{90} of **Ir1** against *S. aureus* was 3.13 μmol/L while there was no obvious inactivation ability toward

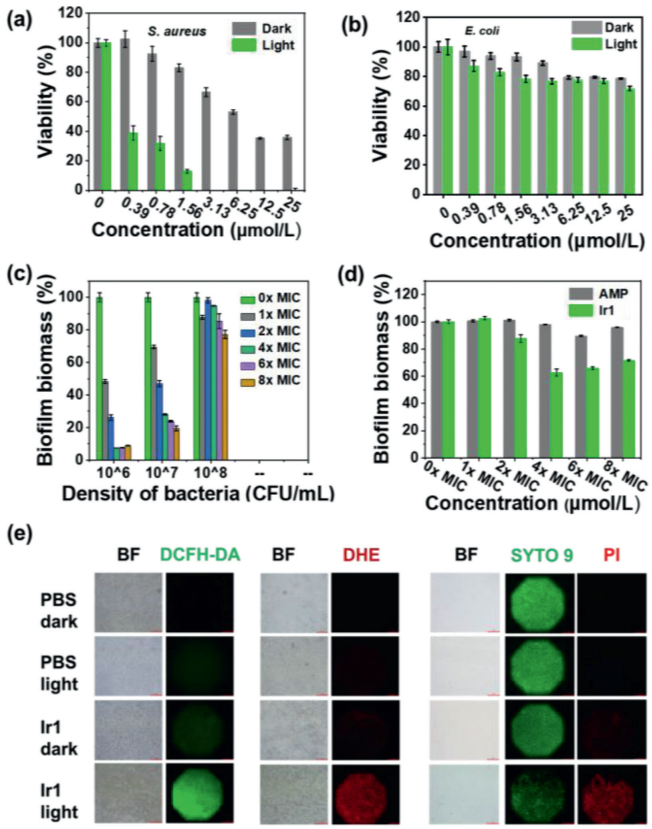

Fig. 2. Photo-inactivation of *S. aureus* (a) and *E. coli* (b) with **Ir1** under white light (21.1 J/cm^2). (c) Biofilm formation inhibition experiments, and *S. aureus* are incubated with **Ir1** for 44 h after 21.1 J/cm^2 white light treatment. (d) Mature biofilm destruction experiments, and mature *S. aureus* biofilm are incubated with **Ir1** for 3 h after 21.1 J/cm^2 white light treatment. (e) The first two pictures are ROS and superoxide anion produced in bacteria of biofilm treated with various conditions, detected by DCFH-DA and DHE. On the right is *S. aureus* biofilm staining with SYTO 9 and PI.

Table 1
MIC_{90} values of complexes towards *S. aureus* and *E. coli*.

Complexes	*S. aureus*		*E. coli*	
	MIC_{90}[a] (Dark)	MIC_{90}[b] (Light)	MIC_{90}[a] (Dark)	MIC_{90}[b] (Light)
Ir1	>25	3.13	>25	>25
Methicillin	6.25	6.25	>25	>25
Streptomycin	>25	>25	>25	>25
Ampicillin	3.13	1.56	25	25

[a] The bacteria incubated with **Ir1** or antibiotics in the dark for 18 h.
[b] The bacteria incubated with **Ir1** or antibiotics in the dark for 4 h, then exposed to white light irradiation for 20 min (17.6 mW/cm^2) and finally incubated for another 14 h. The unit of MIC_{90} is μmol/L.

Gram-negative bacteria. Notably, **Ir1** also exhibited obvious dark toxicity against *S. aureus*. These results illustrated that **Ir1** exhibited synergistic effects against *S. aureus*, functioning as chemotherapeutic agent in the dark and phototherapeutic agent upon light activation. The dark and light MIC_{90} values of **Ir1** and several clinical antibiotics were summarized in Fig. S8 and Table 1. Moreover, light MIC_{90} of **Ir1** against *S. aureus* reaches to 1.56 μmol/L when administrated with 3-fold intensity of light power (63.3 J/cm^2, Fig. S10 in Supporting informaton), indicating excellent photo-stability of **Ir1** and the antimicrobial activity can enhance *via* increasing the light dose. Since the fact that low light dose can decrease side effects, further experiments were performed with white light power of 21.1 J/cm^2.

Bacteria can generate biofilm, a stronger barrier, to protect themselves from antibiotics. As a result, though the clinical used antibiotics exhibit strong antimicrobial activity toward bacteria, the therapeutic effect will be significantly inhibited treating with biofilm. Given the excellent activity of **Ir1** against *S. aureus*, the capability of biofilm destruction was further investigated. We employed the crystal violet staining to explore the efficacy of biofilm inhibition and biofilm destruction, respectively [26]. The inhibition of biofilm formation was detected 44 h after dark or light treatment with *S. aureus* at 37 °C. As shown in Fig. 2c, the inhibition efficiency of biofilm formation strongly depends on the density of bacteria (10^6–10^8 CFU/mL) and the dose of **Ir1**. For 10^6 CFU/mL *S. aureus*, 4× MIC_{90} concentration of **Ir1** can inhibit ~90% of biofilm biomass upon light irradiation. When the bacterial density increased, **Ir1** can still inhibit biofilm formation but was less effective than ampicillin (Fig. S11 in Supporting informaton). It is important to mention that ampicillin exhibited inconspicuous mature biofilm elimination capability (Fig. 2d), which promoted us to investigate the mature *S. aureus* biofilm destruction ability of **Ir1**. As shown in Fig. 2d, **Ir1** can effectively damage the mature *S. aureus* biofilm (destruction rate, ~35%–40%, over 4× MIC_{90} concentration) after white light treatment.

The excellent ability of **Ir1** towards both inhibition of biofilm formation as well as the mature biofilm destruction promoted us to further investigate the potent mechanism of action towards *S. aureus*. Firstly, the positive-charged nature of **Ir1** may enhance the drug interaction with the negatively charged bacterial membrane. In order to figure out the interaction mode, we measured the change of zeta potential of *S. aureus* surface. However, the zeta potential of *S. aureus* just changed slightly in the presence or absence of **Ir1** (Fig. 3a). Thus, **Ir1** did not locate at the surface of bacteria due to negligible impact on zeta potentials change of the bacteria [27,28]. Considering the inconspicuous change of zeta potential of *S. aureus* and strong inactivation effect of **Ir1**, it is expected that **Ir1** was able to insert into the poriferous cell wall of *S. aureus*. Besides, ROS produced in biofilm is able to destroy component of biofilm containing DNA, proteins, lipids, polysaccharide, *etc*. As expected, **Ir1** can provide ROS upon biofilm, causing significant death of *S. aureus* biofilm (Fig. 2e). Herein, ROS is very important for biofilm destruction, which may explain why ampicillin exhibits low effect on biofilm.

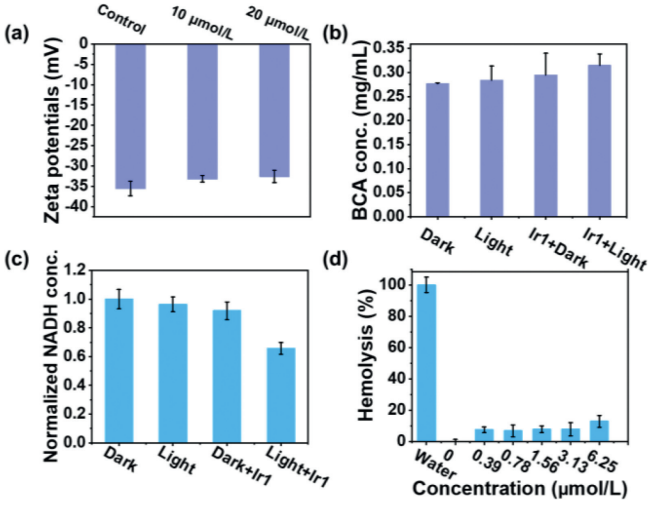

Fig. 3. (a) Zeta potentials of *S. aureus* in H_2O pretreated with or without **Ir1** for 60 min. (b) BCA released from bacteria following receiving various treatments. The amount of BCA released from **Ir1**-treated bacteria *versus* from that of other formulations-treated bacteria. (c) NADH deletion within *S. aureus* following receiving various treatments. (d) Hemolysis test results of **Ir1**.

Subsequently, the enhanced bicinchoninic acid (BCA) protein assay kit was employed to evaluate the bacterial cell membrane integrity after treatment [26]. As shown in Fig. 3b, the BCA protein released from **Ir1** and light treated group was higher than the other groups, indicating that a certain degree of bacterial cell membrane was ruptured after treatment. Additionally, NADH in *S. aureus* was also eliminated effectively when bacteria incubated with **Ir1** was irradiated with white light (21.1 J/cm^2) (Fig. 3c).

Hemolysis, which involves the disruption of erythrocyte membranes, is an obstacle for potent pre-clinical compounds. We explored the hemolysis of **Ir1** preliminary by treating 10% erythrocyte stock solution with diverse concentrations of **Ir1** (0–6.25 μmol/L). As shown in Fig. 3d, **Ir1** caused less than 10% hemolysis after 1 h of incubation at 37 °C, suggesting that **Ir1** exhibited high biocompatibility.

Compare with Ir(III) photocatalysts published previously [20,21,24,25,29], we may conclude the structure activity relationship that Ir(III) photocatalysts with bis-tridentate system can significantly extend the light absorption wavelength as well as enhance the molar extinction coefficient. Thus, bis-tridentate Ir(III) photocatalysts may be a suitable platform to develop long wavelength light excited Ir(III) photocatalyst for the treatment of bacterial infection in deep tissue. However, it should also be concerned that multiple side product may occur during synthesis which results in low synthetic yield due to the high reaction temperature (200 °C).

In summary, we designed and synthesized a novel bis-tridentate Ir(III) photocatalyst and evaluated the antimicrobial photodynamic therapy activity. **Ir1** generated diverse ROS and induced photocatalytic oxidation of NADH upon low-dose white light irradiation. **Ir1** exhibited excellent *S. aureus* inactivation activity *via* synergistic type I and type II mechanisms of action. Additionally, **Ir1** showed promising biofilm formation inhibition and mature biofilm destruction activity, indicating relatively low antimicrobial drug resistance. The antibacterial and anti-biofilm mechanisms of **Ir1** may be attributed to high lipophilicity, excellent photocatalytic ROS production and NADH oxidation activity. These results suggest that **Ir1** may be a promising antimicrobial PDT candidate for the treatment of Gram-positive bacterial infection. As one of the few studies about iridium complexes for antimicrobial PDT, this work would further facilitate the exploration of transition metal antibacterial materials to combat the severe bacterial infection.

Declaration of competing interest

The authors declare that they have no known competing financial interests or personal relationships that could have appeared to influence the work reported in this paper.

Acknowledgments

This work was financially supported by the “Summit Plan” High-Level Hospital Construction Project of Foshan (No. FSSYKF-2020002), the Medical Scientific Research Projects of Foshan Health Bureau (No. 20210358), the National Natural Science Foundation of China (NSFC, Nos. 22277153, 22007104), Guangdong Basic and Applied Basic Research Foundation (No. 2021B1515020050), Science, Technology and Innovation Commission of Shenzhen Municipality Project (No. JCYJ20190807152616996) and the Fundamental Research Funds for the Central Universities (No. 22lgqb37).

Supplementary materials

Supplementary material associated with this article can be found, in the online version, at doi:10.1016/j.cclet.2023.108412.

References

[1] G.A. Durand, D. Raoult, G. Dubourg, Int. J. Antimicrob. Agents 53 (2019) 371–382.
[2] M.Y. Cao, Z.S. Chang, J.S. Tan, et al., ACS Appl. Mater. Interfaces 14 (2022) 13025–13037.
[3] A.S. Lee, H. Lencastre, J. Garau, et al., Nat. Rev. Dis. Primers 4 (2018) 18033.
[4] L.N. Xie, Z.D. Luo, Z.N. Zhao, et al., J. Med. Chem. 60 (2017) 202–214.
[5] Z.N. Zhao, P. Gao, L. Ma, et al., Chem. Sci. 11 (2020) 3780–3789.
[6] M.K. Chen, X.T. Huang, J. Lai, et al., Chin. Chem. Lett. 32 (2021) 158–161.
[7] J.J. Li, H.J. Luo, X.Q. Zhu, et al., Chin. Chem. Lett. 33 (2022) 788–792.
[8] F.F. Li, J.G. Collins, F.R. Keene, Chem. Soc. Rev. 44 (2015) 2529.
[9] A.K. Gorle, M. Feterl, J.M. Warner, et al., Dalton Trans. 43 (2014) 16713.
[10] F. Chen, J. Moat, D. McFeely, et al., J. Med. Chem. 61 (2018) 7330–7344.
[11] A. Gupta, P. Prasad, S. Gupta, et al., ACS Appl. Mater. Interfaces 12 (2020) 35967–35976.
[12] Q.Y. Jia, Q. Song, P. Li, et al., Adv. Healthc. Mater. 8 (2019) 1900608.
[13] J. Hynek, J. Zelenka, J. Rathousky, et al., ACS Appl. Mater. Interfaces 10 (2018) 8527–8535.
[14] D.O. Frimannsson, M. Grossi, J. Murtagh, et al., J. Med. Chem. 53 (2010) 7337–7343.
[15] M.M. Kang, C.C. Zhou, S.M. Wu, et al., J. Am. Chem. Soc. 141 (2019) 16781–16789.
[16] N.A. Smith, P.Y. Zhang, S.E. Greenough, et al., Chem. Sci. 8 (2017) 395.
[17] P.Y. Ho, S.Y. Lee, C. Kam, et al., Adv. Healthc. Mater. 10 (2021) 2100706.
[18] A. Chiarugi, C. Dölle, R. Felici, et al., Nat. Rev. Cancer 12 (2012) 741–752.
[19] A. Sil, U. Ghosh, V.K. Mishra, et al., Inorg. Chem. 58 (2019) 1155–1166.
[20] H.Y. Huang, S. Banerjee, K.Q. Qiu, et al., Nat. Chem. 11 (2019) 1041–1104.
[21] C. Huang, C. Liang, T. Sadhukhan, et al., Angew. Chem. Int. Ed. 60 (2021) 9474–9479.
[22] X. Yang, J. Li, T. Liang, et al., Nanoscale 6 (2014) 10126–10133.
[23] M. Yazdani, Toxicol. In Vitro 30 (2015) 578–582.
[24] Z.X. Fan, J.E. Xie, T. Sadhukhan, et al., Chem. Eur. J. 28 (2022) e02103346.
[25] Z.X. Fan, Y. Rong, T. Sadhukhan, et al., Angew. Chem. Int. Ed. 61 (2022) e202202098.
[26] J.W. Zhu, J. Tian, C. Yang, et al., Small 17 (2021) e2101495.
[27] H.X. Yuan, Z. Liu, L.B. Liu, et al., Adv. Mater. 26 (2014) 4333–4338.
[28] H.T. Bai, H.X. Yuan, C.Y. Nie, et al., Angew. Chem. Int. Ed. 54 (2015) 13208–13213.
[29] L. Wei, R. Kushwaha, A.Y. Dao, et al., Chem. Commun. 59 (2023) 3083–3086.